-RESEARCH PAPER-

International Journal of Mining and Geo-Engineering

IJMGE

IJMGE 57-2 (2023) 223-229

DOI: 10.22059/IJMGE.2023.353554.595019

Investigating mechanical and geometrical effects of joints on minimum caving span in mass caving method

Behnam Alipenhani [a], Abbas Majdi [a] and Hassan Bakhshandeh Amnieh [a, *]

[a] *School of Mining Engineering, College of Engineering, University of Tehran, Tehran, Iran.*

Article History:

Received: 07 January 2023.

Revised: 03 March 2023.

Accepted: 22 May 2023.

ABSTRACT

This paper investigates the effect of jointed rock mass properties on the Minimum Required Caving Span (MRCS) in the block caving method using numeric and heuristic approaches. To do so, the effects of five parameters of jointed rock mass, namely joint set number, joint spacing, joint inclination angle, joint surface friction angle, and undercut depth on MRCS, were investigated using a discrete element code. For this purpose, many numerical models were generated with various rock mass parameters. Moreover, Gene Expression Programming and Artificial Neural Networks were employed to create a heuristic model for MRCS. The model parameters were subjected to sensitivity analysis. All model input parameters showed sensitivity to the model. There are several effective parameters on MRCS, but joint dip and joint set numbers are the most important and the smallest.

Keywords: *Mass caving, Numerical modeling, Sensitivity Analysis, DEM, GEP, ANN.*

1. Introduction

The block caving method is an underground mining approach that can compete with open-pit mining methods because of its low operating costs and large mining scale. The advantages of this method are the high level of safety for personnel and the ability to use automation. Due to the decreasing rate of current open pit mine deposits and the increasing industrial demands for minerals, especially copper and iron, and because of the benefits of the block caving method, the mining industry has paid specific attention to the adoption of this large-scale approach. A prerequisite for applying this approach is cavability, one of the essential factors in block caving mining [1]. Rock mass caveability under certain conditions must be measured for the initiation, propagation, and continuity of caving [2]. The adoption of reliable approaches to predict caveability and the possibility of applying this method at the initial design stage is an essential demand. Not only do the results of caving studies affect the design and cost of exploitation, but they also impact the cost of secondary blasting, loading, and even processing operations [3]. The initiation of the caving process and its propagation during mining activity are crucial factors due to their impact on a mine's production and economic considerations [4]. Many researchers have adopted analytical, empirical, and numerical approaches to investigate the caveability of jointed rock mass [5-31].

The analytical method was used to investigate the behavior of caving propagation in a two-dimensional mode. This method considered assumptions, but later studies showed that these assumptions were incorrect. Also, in these methods, the geomechanical parameters of the rock mass were not considered. Empirical methods that use various rock mass classification systems have limitations, such as the dependence on personal opinion for selecting index value (RQD [32], MRMR [33,34], Q, N [35]), and the dependence of the results on input data accuracy. Numerical methods can simulate the caving of rock mass in complex geological conditions. The history of these methods, along with their advantages and disadvantages, has been explained by Alipenhani et al [36-39]. In this paper, the minimum caving span is determined using numerical modelling results. Several parameters were considered, including joint spacing, dip, angle of friction, and undercut depth. Gene Expression Programming was adapted to create a heuristic model to predict the Minimum Required Caving Span (MRCS) based on the input parameters. Each parameter of the MRCS model was subjected to multiple parameter sensitivity analysis (MPSA).

Calculating the minimum caving span through a mathematical formula is an important issue that has not been investigated so far. However, in their paper, Alipenhani et al. obtained a simple relationship to calculate this variable using multivariate regression. In this paper, using the GEP algorithm, a new relationship for calculating the minimum caving span is presented.

2. Methods

This paper adopts a combination of numerical, heuristic, and statistical approaches to investigate the caveability of the jointed rock mass. For this purpose, through a discrete element code, numerical models were generated, and the effect of each parameter of the jointed rock mass on MRCS was investigated. Then, the GEP modelling was employed to create a heuristic model. Finally, the sensitivity analysis was done on the model output to determine the effect of each rock mass parameter on MRCS.

2.1. Numerical Simulation

In this research, to investigate the effect of discontinuity parameters on MRCS, the Distinct Element software was used to model the block caving process. Two-dimensional modelling can improve calculation speed and include more details about the geotechnical characteristics of the rock mass. As shown in Figure 1, the model's height is 350 meters,

* Corresponding author. Tel: (+98-021)82084141, *Fax*: (+98-21)88008838, *E-mail address:* hbakhshandeh@ut.ac.ir (H. Bakhshandeh Amnieh).

and its width is 1000 meters (to avoid the influence of boundaries on the results). The numerical model is divided into two areas with and without joints to save running time.

A jointed area and an unjointed area of the model were divided to save time (mesh lengths 0.5 m and 10 m, respectively). The model was wide (4.5 times the maximum span created) to prevent the effect of boundary conditions on the result. This geometry is used to reduce computational time. The characteristics entered in the model are similar to the values used by Alipenhani et al.

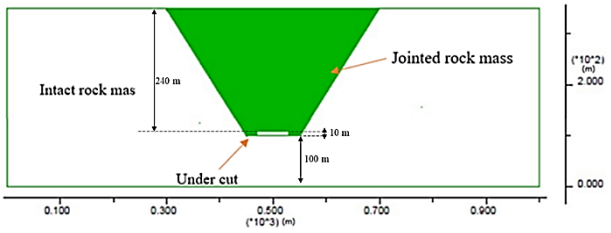

Figure 1. The numerical model of block caving operation.

2.2. Gene Expression Programming (GEP)

In 1999, the GEP method was formulated and introduced by Ferreira [40]. To correct the GP trees, plain chromosomes and sprouted configurations of different sizes and shapes were combined.

A schematic view of the main steps in this method is shown in Figure 2a. The suitability of the attained score is rechecked through the criteria. Modelling is complete at this point, and the information obtained from the model is encoded for the best solution [41-44]. There are five main steps in GEP modelling, as shown in Figure 2b. [40].

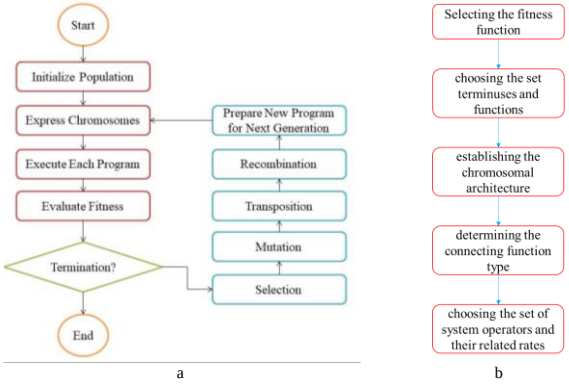

Figure 2. a) The schematic view of the GEP algorithm process; b) main steps in GEP modelling [45,46].

2.3. Multiple regression analysis

Multiple Linear Regression (LR) analysis is a statistical approach to predict the values of one or more dependent variables from a wide array of (independent) variables [47-50]. LR models have been adopted to forecast MRCS. Generally, multiple regression models are shown by the following equation:

$$y = \beta_0 + \beta_1 X_1 + \ldots + \beta_k X_k + e \quad (1)$$

where y is the response variable whose outcome depends on the predictor variables (x_1, x_2, ... x_k), chosen by the examiner, and 0, ... k are regression parameters [51-53]. To describe the predicted value of y in this context, the following formula is applied:

$$y^* = x(x'x)^{-1}x' \quad (2)$$

The residuals are defined as:

$$e = y - y^* \quad (3)$$

3. Modeling

3.1. Numerical simulation process

Numerical modelling steps include solving the elastic model, applying gravity stress, and applying the Mohr-Coulomb criteria to the rock mass and joints. The boundary conditions of the model are shown in Figure 1. Undercuts are excavated in 2-meter steps from the center of the model. Then the caved material is removed from the model, and the run continues. The caving criterion was considered displacement greater than or equal to 1 meter. Figures 3 and 4 show the displacement counter in the first and last stages of drawing, respectively.

3.2. Gene Expression Programming Modeling

This part aims to establish an optimum GEP model to predict MRCS. In GEP modelling, access to an enriched database is mandatory to achieve proper results. Based on the numerical analyzes discussed in Section 3.1, about 480 data sets were arranged in the GEP model to invent the best relationship for MRCS assessment.

The datasets were arbitrarily divided into test (30 percent) and train datasets (70 percent). The test datasets were not applied to the models in the training phase, but they were used for testing and validation. Five influential input variables, including joint set number (JN), joint spacing (JS), joint inclination angle (JI), joint surface friction angle (JF), and undercut depth (UD), were considered. Table 1 shows the statistics of the input and output variables of the GEP model and their symbols.

The MRCS prediction was performed employing the GEP approach in five basic steps. In the first step, the fitness function should be selected. In this paper, root-relative standard error (RRSE) was selected as the optimum fitness function. The second stage is to choose the set of terminals (T) and functions (F). The influential parameters mentioned in the model determine the terminal sets. In addition, the nature of the problem governs the selection of the function sets. In this study, the terminal set, including joint set number (JN), joint spacing (JS), joint inclination angle (JI), joint surface friction angle (JF), and undercut depth (UD), was used for the MRCS estimate. Additionally, basic functions that contained the operators, such as plus, minus, multiplication, and division, and Logarithmic, power, trigonometric and radical functions were used. The third, fourth, and fifth primary phases are carried out according to Figure 2b.

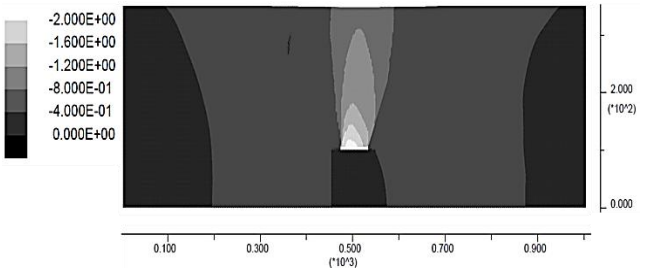

Figure 3. Displacement contours in the numerical model (Span = 60m).

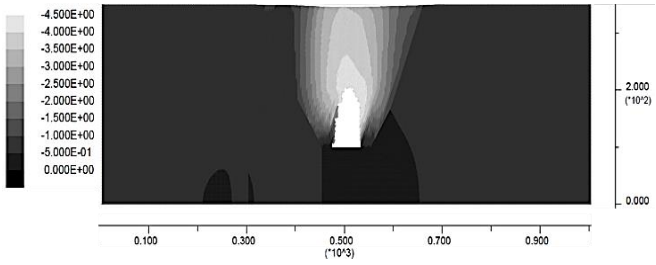

Figure 4. Displacement contours in the final step.

The GeneXproTools 5 software was utilized to determine the values related to these steps through trial and error. A wide variety of

parameters were used for the GEP models, and the best one was chosen according to the least values of RMSE. The best parameters operated in the model are presented in Table 2 and Table 3. It is obvious from the tables that the least error has resulted from the GEP model with the addition of the linking function and type 5 operators.

Table 1. Statistics of the input and output variables of the GEP model and their symbols.

Type	Parameter	Symbol	Unit	Min.	Max.
Input	Joint set Number	JN	-	2	3
	Undercut Depth	UD	m	50	400
	Joint Spacing	JS	m	1	5
	Joint Friction angle	JF	Degree	10	40
	Joint Inclination	JI	Degree	25	70
Output	Minimum required caving span	MRCS	m	2	98

Table 2. Optimum parameters in the GEP modeling used for prediction.

factor	amount
Number of chromosomes	30
Head size	8
number of Gene	5
Mutation rate	0.00133
Inversion rate	0.00545
One point recombination rate	0.00277
Two-point recombination rate	0.00277
Gene recombination rate	0.122
Gene transposition rate	0.1
IS transposition rate	0.2
Transposition of RIS	0.2
Constant for each gene	3

Table 3. Comparison of RMSE values for numerous functions in the MRCS prediction.

Operator type	Definition	RMSE
1	$\{+,-,\times,\div\}$	0.124
2	$\{+,-,\times,\div, lnx, e^m\}$	0.365
3	$\{+,-,\times,\div, x, \sqrt[3]{x}, x^2, x^3\}$	0.425
4	$\{+,-,\times,\div, e^x, lnx, \sqrt{x}, \sqrt[3]{x}, x^3, x^2\}$	1.582
Linking functions		
Addition		0.025
Multiplication		0.018
Subtraction		0.017
Division		0.025

Based on the proper functions and parameters in Tables 2 and 3, the training and testing fitness of the best model resulted in 912.72 and 926.48, respectively. Figure 5 shows the expression tree of the best models (GEP) to foresee MRCS. The indexes 3d0, d1, d6 m d7, and d8 refer to a joint set number (JN), undercut depth (UD), joint spacing (JS), joint surface friction angle (JF), joint inclination angle (JI), respectively. Moreover, in each sub-ET, c0 and c3, c4, c5, c6, and c8 are the constant factors mined from the GEP model output. Finally, the ultimate function based on the best GEP procedures to forecast the MRCS was obtained as Eq. (1).

$$MRCS = [Arc\,cot(0.0025 - \sqrt[3]{JI}) + (\sqrt{ln(JF)})] + \frac{JN/2.45}{e^{3.25-\sqrt{JS}}}$$
$$\times [sin(Arc\,tan((6.41JF - ((ln(JS - 0.11)) \times UD))))] \quad \text{(Eq. 1)}$$

Mean absolute error (MAE), correlation coefficient (R), and relative root standard error (RRSE) criteria were used to evaluate the performance of the models. As can be seen in Table 4, the values obtained from the indices in both stages (high R-value and low RRSE and MAE) confirm the very good performance of the GEP model in predicting MRCS.

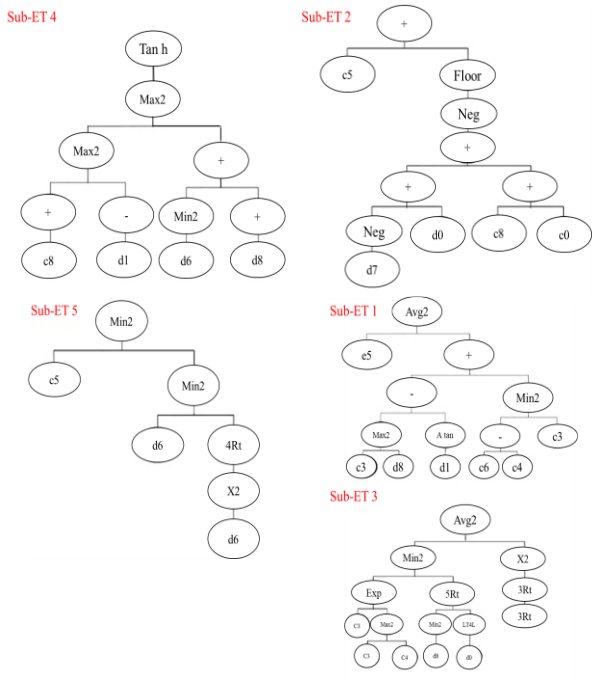

Figure 5. The corresponding expression tree.

Table 4. Statistical indices calculated for the GEP model in the training phase for MRCS estimation.

Statistical Index	GEP model
R^2	0.9487
MAE	0.011822239
RMSE	0.00000831

Moreover, a comparison has been carried out in Fig 6 between the predicted and simulated MRCS. As shown in this figure, there is an excellent agreement between the predicted and simulated values in both phases of the proposed model.

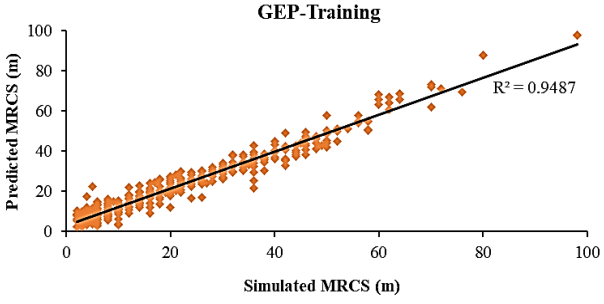

Figure 6. Comparison between values obtained from the numerical simulation and predicted from the GEP models in the training phase.

Finally, the correlation between the suggested GEP model outcomes and the target MRCS value in the training phase is shown in Fig 7. From the diagram, it can be concluded that the proposed model can predict MRCS in the block-caving method with high confidence.

3.3. Linear Regression Modeling (LR)

To predict the MRCS, efforts were made to employ conditions to solve the issue of providing a line by the smallest square. The coefficient of F was adopted to evaluate the statistical significance of the regression model, assuming that the same data is employed for GEP training. To do so, the collected datasets were arbitrarily divided to test (30 percent) and train datasets (70 percent), and the model was derived from the training data. The analysis of variance for the MRCS model is presented in Table 5.

Table 5. The results of variance analysis for LR.

Model	Sum of Squares	df	Mean Square	F	Sig.
Regression	116227.49	5	23245.4	159.92	0
Residual	69190.562	476	145.35		
Total	185418.052	481			

Statistical indices calculated for the LR model in the training phase for the MRCS estimation are shown in Table 6. The best regression model for MRCS is given in Eq. 2.

$$MRCS = -8.659 - 5.903 \times JN - 0.036 \times UD + 5.661 \times JS + 1.028 \times JF + 0.155 \times JI \quad \text{(Eq. 2)}$$

3.4. Artificial neural network (ANN)

ANN is a branch of artificial intelligence, including a multilayer topology with interconnected layers. In the first layer, inputs are placed, while outputs are placed in the last layer. Besides the mentioned layers, one or more layers, called hidden layers, are located between the first layer (input) and the last layer (output). The components of the hidden layers, termed neurons conduct the needed computations. A try-and-error approach determines the number of the hidden layer's neurons. When there is a very low correlation, the best solution is ANN compared to the present conventional alternatives [50]. Among the different benefits of ANN modelling, function approximation, and feature selection are regarded as particular capabilities [54].

It is required to collect an adequate number of datasets (a set of inputs and corresponding outputs) and use them for training different network architectures from which the best combination is chosen. In this process, a random weight would be first assigned to the connections between the neurons. Then, the initially set weights are updated in each modelling run to obtain the best possible network with the highest efficiency. An appropriate training approach should be adopted in the next step, like a backpropagation algorithm with significant benefits compared to other available methods [54].

To train and test the groups, a total of 480 datasets were utilized in the present work. The model training was done by a backpropagation method. All datasets were normalized in the interval of -1 and 1 to have an applicable database and to improve the training process efficiency. Following preprocessing of the datasets, the best possible model with the lowest error and the highest accuracy was found by creating many networks with various related elements, including the number of hidden layers and their corresponding neurons [50]. The results indicate the best model as a backpropagation network with a 5-28-1 architecture, an exponential transfer function in the output, and a Logistic function in the hidden layers (No.1). Figure 7 also indicates the optimal architecture of the ANN model. The calculated R2 was 0.98, which is enough to show the competency of the presented ANN model.

4. Discussion

4.1. Comparative study

Based on the test data, a comprehensive comparative analysis was conducted between the performance of three models (GEP, LR, and ANN). Some statistical indices, such as R, MAE, and RRSE, were employed to assess the performance of the models. The calculated values for both models are presented in Table 8. Table 7 shows the acceptable performance of all models. However, the reliability of the ANN model is better than the GEP model and linear regression model. Also, the accuracy of the GEP model in estimating MRCS is much higher than the LR model. For better evaluation and conformation, the correlations between the models by the simulated data are shown in Fig. 8. It can be inferred that the GEP model has a better correlation with the simulated data than the LR model. Finally, an evaluation of the results of the model with the simulated MRCS is shown in Figures 9-11. These figures indicate good conformity between the results of the models and the simulated MRCS. Moreover, the results of the ANN model have a better agreement with the numerical simulation results than the results of the GEP and LR models. In many conclusions, the ANN and GEP models can be applied as precise techniques, and the linear regression model may be utilized for issues where high accuracy is not required.

Table 6. The statistical indices calculated for the LR model in the training phase for the MRCS estimation.

Statistical Index	GEP model
R^2	0.87
MAE	0.54
RMSE	0.039

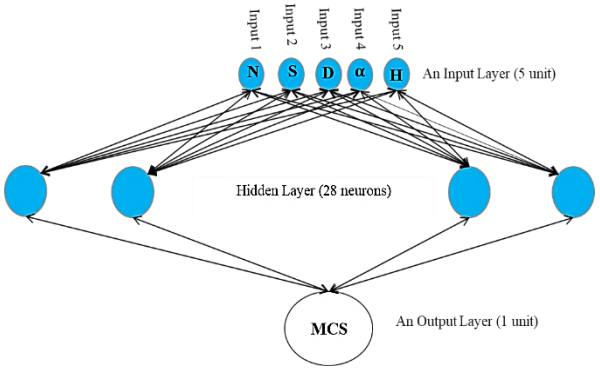

Figure 7. The optimal ANN model architecture.

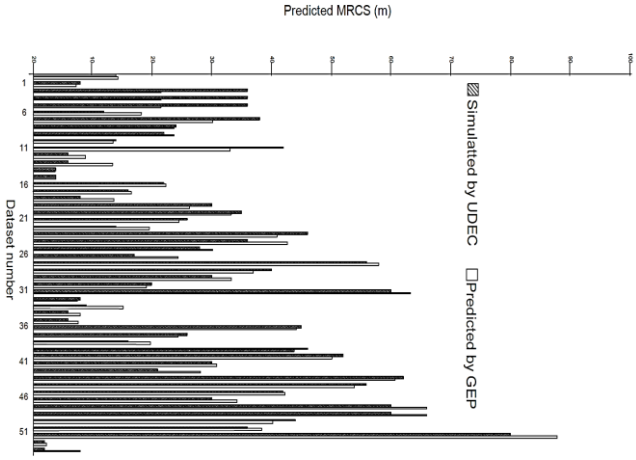

Figure 8. The graph of the results of the GEP model according to the values obtained from the numerical simulation.

Table 7. The statistical indices of models used in MRCS assessment.

type of index	MRCS assessment		
	GEP	ANN	LR
R^2	0.9511	0.98	0.82
MAE	1.180579647	2.13	0.45
RRSE	0.00372361	0.054	0.32

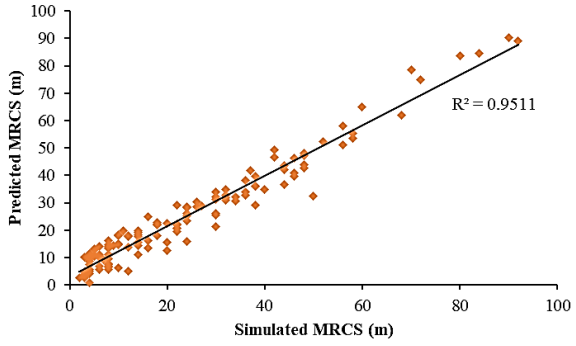

(a) GEP model

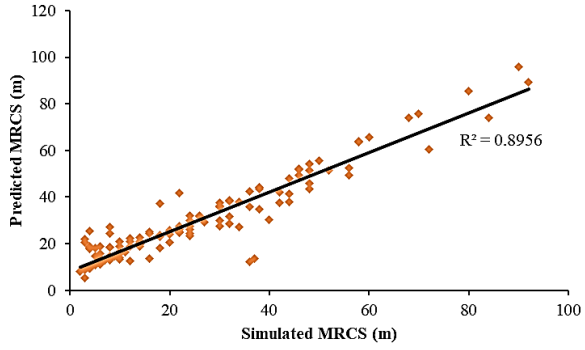

(b) LR model

Figure 9. The correlation of the model's results a) GEP and b) LR with the determined values.

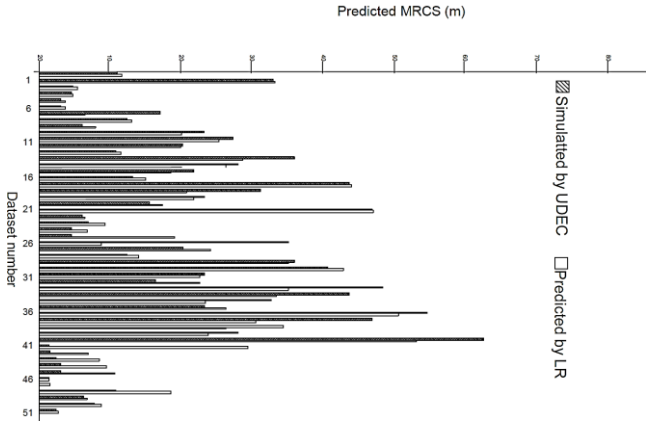

(a) GEP model

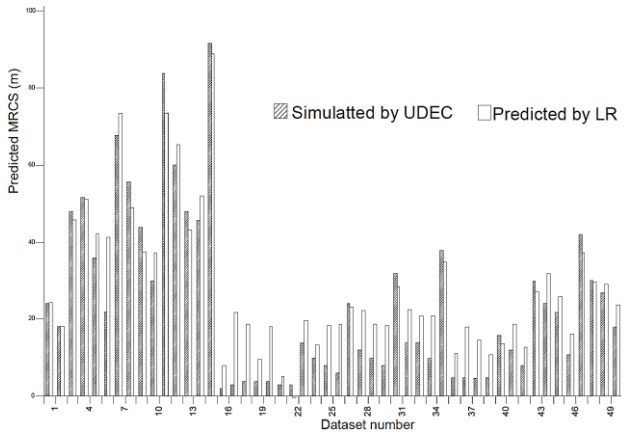

Figure 10. The results of the GEP model and liner regression against simulated MRCS.

Table 8. The equation used in MPSA

Equation	No.
$F_l = \sum_{l=1}^{n} [y_{0,l} - y_{d,l}(j)]^2$	(11)
$\delta_l = \frac{f_l}{x_{0,l}}$	(12)
$\gamma = \sum_{l=1}^{j_{MRCS,max}} \delta_l$	(13)

F_l: objective function value for a given MRCS variable l;

$y_{0,l}$: its observed value;

$y\,j)_{d,l}$: calculated value y_d for each input series;

n: the number of variables contained in the random series;

l: each pair entry, the results were obtained for each evaluated parameter by applying the method described in the MRCS model;

in equation 6: MRCS is evaluated from l=1 to the maximum value ($j_{MRCS,max}$); and

γ: indicates the importance of the parameter.

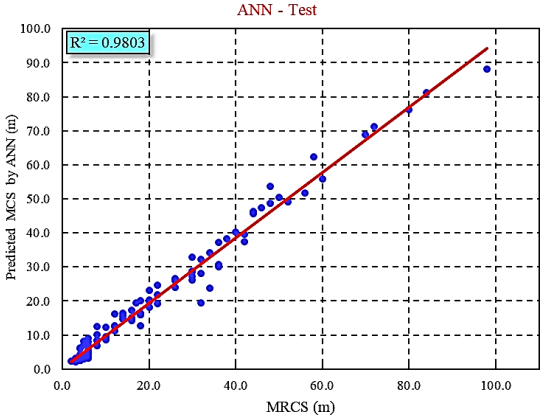

Figure 11. The scatter plot of actual versus predicted MRCS for Artificial neural network method.

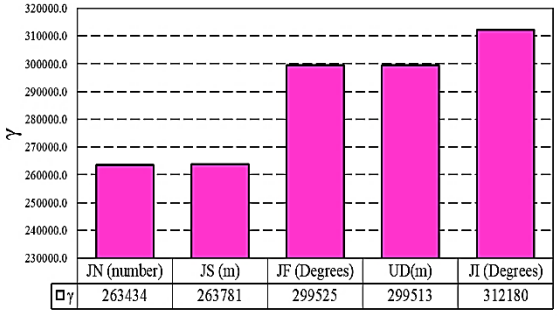

Figure 12. The effect of each parameter on MRCS.

5. MPSA (Multiple Parametric Sensitivity Analysis)

To determine the minimum caving span, the output results of the GEP model were analyzed to determine which parameters had the greatest impact. The first step in this process is to select a parameter for testing. After that, a range is set. For each parameter, a series of independent and random numbers is generated with a normal distribution. In equation 11, the objective function is calculated using the selected series and the trained model. Equation 12 calculates the relative importance of each parameter. Equation 13 also evaluates parametric sensitivity [53].

The higher the γ value, the more sensitive the output variable is to

that parameter. The γ value has three categories, including Insensitive for γ values less than or equal to 1, Sensitive for values between 1 and 100, and highly sensitive for values above 100.

Figure 12 shows the values of γ for the MRCS model. As is apparent in Figure 11, the MRCS model is sensitive to all five investigated parameters. The JI and JN parameters have the most significant and minor influence on the MRCS model, respectively. It can be concluded that JN and JS, as well as UD and JF, have virtually the same effect on MRCS.

6. Conclusion

Using numerical simulations, the MRCS in a rock mass was estimated by GEP-based equations, artificial neural networks, and statistical models (LR models). To compare the results with the numerical model, a new GEP-based equation was evaluated using R^2, MAE, and RMSE indices. This comparison shows that the proposed equation (using GEP) performs better than the statistical model. ANNs perform better than GEPs, but their performances are very similar.

Also, the results obtained from the proposed GEP model are in agreement with those obtained from the numerical simulation. A sensitivity analysis of parameters affecting the MRCS was conducted in the end. According to the obtained results, the MRCS was sensitive to all selected parameters. Among these parameters, JI and JN have the most and minor effects on the MRCS model, respectively. It can also be concluded that JN and JS, as well as UD and JF, have virtually the same effect on MRCS.

REFERENCES

[1]. Brady BHG, Brown ET (2004) Rock mechanics and mining engineering. In: Rock Mechanics for underground mining. Springer Netherlands, Dordrecht, pp 1–16.

[2]. Mawdesley CA (2002) Predicting rock mass caveability in block caving mines, (October), p. 436.

[3]. Kendorski F (1978) The Caveability of ore deposits. Min Eng., vol. 30, No6, Jun.

Charles A. Brannon, Gordon K. Carlson, Casten TP (2011) Block Caving & Cave Mining. SME Mining Engineering Handbook Nework. p 49.

[4]. Rice G (1934a) Ground movement from mining in Brier Hill mine. Min Metall 15:12–14.

Palma R, R A (1973) A Study of the Caveability of Primary Ore at the El Teniente Mine. In: Technical Report from Colombia University, NY.

[5]. Mathews KE, Hoek E, Wyllie DC, Stewart S (1981) Prediction of stable excavation spans for mining at depths below 1000 m in hard rock. CANMET DSS Ser No 0sQ80-00081, Ottawa.

[6]. Panek LA (1984a) Subsidence in Undercut-Cave Operations, Subsidence Resulting from Limited Ex-traction of Two Neighboring-Cave Operation. In: Geomechanical.

[7]. Tobie, R.L. and Julin DE (1984) Block Caving: General Description. In: in Underground Mining Methods Handbook, W. A. Hustrulid, ed., Soc. Mng. Enngr, New York, pp 967–972.

[8]. Rech, W., Lorig. L (1992) Predictive numerical stress analysis of panel caving at the Henderson Mine. In: Proc. of MASSMIN. pp 55–62.

[9]. McNearny R., Abel J. (1993) Large-scale two-dimensional block caving model tests. Int J Rock Mech Min Sci Geomech Abstr 30:93–109. DOI: 10.1016/0148-9062(93)90703.

[10]. Laubscher D (2000) Cave Mining Handbook. 1–138.

[11]. Lorig L (2000) The Role of Numerical Modelling in Assessing Caveability. In: Itasca Consulting Group, Inc., Report to the International Caving Study.

[12]. Brown ET (2002) Block caving geomechanics. 696.

[13]. Flores, G and Karzulovic A (2004) Geotechnical Guidelines Subsidence. In: Prepared for International Caving Study, Stage II, JKMRC. Brisbane.

[14]. Ross, I., and van As A 2005. (2005) Northparkes Mines – Design, Sudden Failure, Air-Blast and Hazard Management at the E26 Block Cave. In: Ninth Underground Operators Conference. Perth, WA.

[15]. Mas Ivars D, Pierce ME, Darcel C, et al (2011) The synthetic rock mass approach for jointed rock mass modeling. Int J Rock Mech Min Sci 48:219–244. DOI: 10.1016/j.ijrmms.2010.11.014.

[16]. Carlson G and GJR (2008) Initiation, growth, monitoring, and management of the 7210 caves at Henderson Mine. In: A Case Study in Proceedings of the 5th International Conference and Exhibition on Mass Mining. Lulea University of Technology Press, Lulea, Sweden.

[17]. Beck, D., Sharrock, G. and Capes G (2011) A coupled DFE-Newtonian Cellular Automata scheme for simulation of cave initiation, propagation, and induced seismicity. 45th US Rock Mech Symp Am Rock Mech Assoc.

[18]. Karekal S, Das R, Mosse L, Cleary PW (2011) Application of a mesh-free continuum method for simulation of rock caving processes. Int J Rock Mech Min Sci 48:703–711. DOI: 10.1016/j.ijrmms.2011.04.011.

[19]. Sainsbury B-A (2012) A model for cave propagation and subsidence assessment in jointed rock masses. Univ South Wales.

[20]. Woo KS, Eberhardt E, Rabus B, et al (2012) Integration of field characterization, mine production and InSAR monitoring data to constrain and calibrate 3-D numerical modeling of block caving-induced subsidence. Int J Rock Mech Min Sci 53:166–178. doi: 10.1016/j.ijrmms.2012.05.008.

[21]. Carmichael. P. HB (2012) An investigation into semi-intact rock mass representation for physical modeling block caving mechanic's zone. In: Mining education Australia Research projects review.

[22]. Rafiee R, Ataei M, Khalokakaie R, et al (2015a) Determination and Assessment of Parameters Influencing Rock Mass Caveability in Block Caving Mines Using the Probabilistic Rock Engineering System. Rock Mech Rock Eng 48:1207–1220. DOI: 10.1007/s00603-014-0614-9.

[23]. Rafiee R, Ataei M, KhaloKakaie R, et al (2016) A fuzzy rock engineering system to assess rock mass caveability in block caving mines. Neural Comput Appl 27:2083–2094. DOI: 10.1007/s00521-015-2007-8.

[24]. Rafiee R, Ataei M, KhalooKakaie R, et al (2018) Numerical modeling of influence parameters in cavabililty of rock mass in block caving mines. Int J Rock Mech Min Sci 105:22–27. DOI: 10.1016/j.ijrmms.2018.03.001.

[25]. Wang J., Wei W., Zhang J., Mishra B., and Li A.(2020), 'Numerical investigation on the caving mechanism with different standard deviations of top coal block size in LTCC' , International Journal of Mining Science and Technology, China University of Mining and Technology-Beijing.

[26]. Someehneshin J, Oraee-Mirzamani B, Oraee K (2015) Analytical Model Determining the Optimal Block Size in the Block Caving Mining Method. Indian Geotech J 45:156–168.

doi: 10.1007/s40098-014-0119-1.

[27]. Cumming-Potvin D, Wesseloo J, Jacobsz SW, Kearsley E (2016) Fracture banding in caving mines. J South African Inst Min Metall 116:753–761. DOI: 10.17159/2411-9717/2016/v116n8a7.

[28]. Mohammadi S, Ataei M, Kakaie R (2018) Assessment of the Importance of Parameters Affecting Roof Strata Caveability in Mechanized Longwall Mining. Geotech Geol Eng 36:2667–2682. DOI: 10.1007/s10706-018-0490-2.

[29]. Bai Q, Tu S, Wang F (2019) Characterizing the Top Coal Caveability with Hard Stone Band(s): Insights from Laboratory Physical Modeling. Rock Mech Rock Eng 52:1505–1521. DOI: 10.1007/s00603-018-1578-y.

[30]. Obert, L. E (1973) Design and Stability of Excavation. In: Sec. 7 in SME Mining Engineering Handbook, A. B. Cummins and I. A. Given, ed., Soc. Mng. Enngr, New applications in hard rock mining. Houghton, Michigan, pp 225–240.

[31]. Peter.G. (2011) Selection Process for Hard-Rock Mining. In: 3nd Edition, SME Mining Engineering Handbook, Chapter 6.3. pp 357–376.

[32]. Jakubec J, Esterhuizen (2007) Use of The Mining Rock Mass Rating (MRMR) Classification. In: Proceedings of the International Workshop on Rock Mass Classification in Underground Mining. pp 73–78.

[33]. Suorineni FT (2010) The stability graph after three decades in use: Experiences and the way forward. Int J Mining, Reclam Environ 307–339.

[34]. Vakili A, Hebblewhite BK (2010) A new caveability assessment criterion for Longwall Top Coal Caving. Int J Rock Mech Min Sci 47:1317–1329. doi: 10.1016/j.ijrmms.2010.08.010.

[35]. Brummer RK, Li H, Moss & A, et al The South African Institute of Mining and Metallurgy International Symposium on Stability of Rock Slopes in Open Pit Mining and Civil Engineering the transition from open pit to underground mining: an unusual slope failure mechanism at palabora. 411–420.

[36]. Alipenhani, B., Bakhshandeh Amnieh, H., & Majdi, A., (2023). Application of finite element method for simulation of rock mass caving processes in block caving method. International Journal of Engineering TRANSACTIONS B: Applications. 36 (1), pp. 139-151.

[37]. Alipenhani, B., Majdi, A., and Bakhshandeh Amnieh, H. (2022). Determination of caving hydraulic radius of rock mass in the block caving method using numerical modeling and multivariate regression. Journal of Mining and Environment, doi.org/10.22044/jme.2022.11589.2149.

[38]. Alipenhani, B., Bakhshandeh Amnieh, H., & Majdi, A. (2022). Physical model simulation of block caving in jointed rock mass. International Journal of Mining and Geo-Engineering, 56(4), 349-359.

[39]. Alipenhani, B., Majdi, A., & Bakhshandeh Amnieh, H. (2022). Cavability assessment of rock mass in block caving mining method based on numerical simulation and response surface methodology. Journal of Mining and Environment, 13(2), 579-606.

[40]. Ferreira C (2006) Gene expression programming: mathematical modeling by artificial intelligence.

[41]. Teodorescu L, Sherwood D (2008) High Energy Physics event selection with Gene Expression Programming. Comput Phys Commun 178:409–419. doi: 10.1016/J.CPC.2007.10.003.

[42]. Shakeri, J., Asadizadeh, M., & Babanouri, N. (2022). The prediction of dynamic energy behavior of a Brazilian disk containing nonpersistent joints subjected to drop hammer test utilizing heuristic approaches. Neural Computing and Applications, 34(12), 9777-9792.

[43]. Asadizadeh, M., Babanouri, N., & Sherizadeh, T. (2022). A heuristic approach to predict the tensile strength of a non-persistent jointed Brazilian disc under diametral loading. Bulletin of Engineering Geology and the Environment, 81(9), 364.

[44]. Monjezi, M., Dehghani, H., Shakeri, J., & Mehrdanesh, A. (2021). Optimization of prediction of flyrock using linear multivariate regression (LMR) and gene expression programming (GEP)—Topal Novin mine, Iran. Arabian Journal of Geosciences, 14, 1-12.

[45]. Armaghani DJ, Faradonbeh RS, Rezaei H, et al (2018) Settlement prediction of the rock-socketed piles through a new technique based on gene expression programming. Neural Comput Appl 29:1115–1125. DOI: 10.1007/s00521-016-2618-8.

[46]. Shakeri, J., Asadizadeh, M., & Babanouri, N. (2022). The prediction of dynamic energy behavior of a Brazilian disk containing nonpersistent joints subjected to drop hammer test utilizing heuristic approaches. Neural Computing and Applications, 34(12), 9777-9792.

[47]. Enayatollahi I, Aghajani Bazzazi A, Asadi A (2014) Comparison Between Neural Networks and Multiple Regression Analysis to Predict Rock Fragmentation in Open-Pit Mines. Rock Mech Rock Eng 47:799–807. DOI: 10.1007/s00603-013-0415-6.

[48]. Zhang WG, Goh ATC (2015) Regression models for estimating ultimate and serviceability limit states of underground rock caverns. Eng Geol 188:68–76. doi: 10.1016/J.ENGGEO.2015.01.021.

[49]. Su O (2016) Performance Evaluation of Button Bits in Coal Measure Rocks by Using Multiple Regression Analyses. Rock Mech Rock Eng 49:541–553. doi: 10.1007/s00603-015-0749-3.

[50]. Bayat, P., Monjezi, M., Mehrdanesh, A., & Khandelwal, M. (2021). Blasting pattern optimization using gene expression programming and grasshopper optimization algorithm to minimise blast-induced ground vibrations. Engineering with Computers, 1-10.

[51]. Karakus M, Tutmez B (2006) Fuzzy and Multiple Regression Modelling for Evaluation of Intact Rock Strength Based on Point Load, Schmidt Hammer and Sonic Velocity. Rock Mech Rock Eng 39:45–57. DOI: 10.1007/s00603-005-0050.

[52]. Asadizadeh, M., Karimi, J., Hossaini, M. F., Alipour, A., Nowak, S., & Sherizadeh, T. (2022). The effect of central flaw on the unconfined strength of rock-like specimens: an intelligent approach. Iranian Journal of Science and Technology, Transactions of Civil Engineering, 46(5), 3679-3694.

[53]. Jahanmiri, S., Asadizadeh, M., Alipour, A., Nowak, S., & Sherizadeh, T. (2021). Predicting the contribution of mining sector to the gross domestic product (GDP) index utilizing heuristic approaches. Applied Artificial Intelligence, 35(15), 1990-2012.

[54]. Da Silva, I. N., Spatti, D. H., Flauzino, R. A., Liboni, L. H. B., & dos Reis Alves, S. F. (2017). Artificial neural networks. Cham: Springer International Publishing, 39.